

## Evidence for two-dimensional phonons in a thin metal film

J. C. Nabity and M. N. Wybourne

*Materials Science Institute, University of Oregon, Eugene, Oregon 97403*

(Received 6 May 1991; revised manuscript received 17 July 1991)

In this paper we describe an experiment that uses a moderate dc electric field to heat electrons in a thin metal film that can have its acoustic coupling to the surroundings changed *in situ*. The acoustic coupling is found to have a substantial effect on the electron-heating characteristics. This illustrates the importance of considering phonon escape from the film in this type of experiment. Using a rate equation to model the data obtained for different conditions of phonon escape from the film, we have found that in certain circumstances there is strong evidence to suggest that low-frequency phonons in the film are two dimensional.

### I. INTRODUCTION

A knowledge of the phonon dimensionality in thin metal films has become important for the interpretation of electron-heating experiments,<sup>1-3</sup> yet surprisingly little work has been reported on the subject. The question of phonon dimensionality in thin films is associated closely with the coupling between the phonons in the film and those in the supporting substrate. In the extreme case of a self-supporting film *in vacuo*, phonons of wave vector  $(q_r, q_z)$  will be spatially quantized into subbands according to the criteria  $q_z = n\pi/d$ , where  $d$  is the film thickness in the  $z$  direction and  $n$  is an integer. These subbands will be well defined up to an energy  $\hbar\omega(q)$ , where the inelastic phonon scattering length  $l_i(q) \sim d$ . Phonons above this energy will lose phase memory across the thickness of the film and so will be effectively three dimensional (3D). For the less extreme case of a supported film, an evaluation of the phonon dimensionality is more involved and depends on the acoustic coupling between the film and substrate. If the interface quality is neglected, the relative velocities of sound of the two materials define a critical cone of angle  $\theta_{cr}$  for total phonon reflection; this is Snell's law of refraction applied to acoustic waves.<sup>4</sup> In the general case of an elastically anisotropic solid, each mode will have three critical cones that each have a complex shape in real space. The phonons with  $q_z > q_r/\tan\theta_{cr}$  are within the critical cone and are able to couple to substrate phonons with a coupling coefficient that depends on the relative acoustic impedance of the film and substrate.<sup>5</sup> If the acoustic properties of the film and substrate are not too dissimilar, the acoustic coupling will broaden the subband structure sufficiently to cause the phonons to lose their two dimensional (2D) character. Conversely, phonons with  $q_z < q_r/\tan\theta_{cr}$  are outside the critical cone and undergo total internal reflection within the film as demonstrated recently by Höss, Wolfe, and Kinder.<sup>6</sup> Phonons outside the critical cone experience only weak coupling to the substrate via an evanescent wave. Thus subband broadening will be small and the phonons are expected to be two dimensional if  $l_i(q) > d$ . Several factors may remove the subband structure and increase the

phonon dimensionality. For example, a rough interface will increase the effective critical angle, phonon scattering within the film may change  $q_z$  from less than to greater than  $q_r/\tan\theta_{cr}$ , and frustrated total internal reflection may allow phonon tunneling from the thin film.<sup>6</sup> All three examples provide possible processes for the two-dimensional phonons to leave the film.

While the complexities of a real interface between a metal film and a substrate make details of the phonon dimensionality very difficult to predict, the experimental situation is a little more hopeful. In some recent experiments<sup>3</sup> we showed that it is possible to modify the phonon coupling from a metal film to a substrate *in situ* without cycling the sample to room temperature. This was achieved by having the free surface of a supported metal film either in vacuum or in liquid helium. When in vacuum, the effect of the critical angle will be to lower the dimensionality of some of the phonons in the film. However, when immersed in helium only three-dimensional behavior is expected because the ratio of the metal and helium sound velocities shows that all the phonons are able to couple out of the metal into a small cone in the helium.<sup>7</sup> From the Kapitza effect it is well known that phonon transmission to the helium is much larger than expected from the acoustic impedances of the materials.<sup>8,9</sup> This will further reduce the likelihood of two-dimensional phonons in thin metal films covered with helium.

In the present paper we describe experiments in which a metal film on a silicon substrate is heated by a dc electric field. The electrical resistance of the film as a function of the field is shown to change considerably as the free surface of the film goes from being in a vacuum to being in liquid helium. Furthermore, it is found that the electrical resistance shows distinct features characteristic of the state of the helium in contact with the film. In earlier work<sup>10</sup> we compared the heat loss from metal films deposited on different substrates and we invoked a frequency-dependent acoustic mismatch parameter to describe the data. We have found that this approach is unable to explain the heating characteristics at the higher electric fields used in the present experiments. Using a

rate equation model to describe simultaneously the data obtained under the different surface conditions, we have found that it is necessary to lower the frequency dependence of the phonon density of states, consistent with a reduction of the phonon dimensionality, when the film is in vacuum.

## II. EXPERIMENT

The samples used in this experiment were 25-nm-thick  $\text{Au}_{60}\text{Pd}_{40}$  alloy films. The films were thermally evaporated at a pressure of  $5 \times 10^{-6}$  Torr onto an optically smooth silicon substrate. Before film deposition no attempt was made to remove the oxide layer from the silicon. The samples were  $10 \mu\text{m}$  long and  $1 \mu\text{m}$  wide and were designed<sup>11</sup> for true four-terminal resistance measurements. Their typical sheet resistance was  $R_{\square} = 10 \Omega$ . Resistance measurements were carried out using a low-frequency four-terminal bridge<sup>12</sup> and a signal-averaging technique. With this setup the fractional resistance change could be measured to an accuracy of 5 parts in  $10^7$  with a sensing current of less than  $3 \mu\text{A}$ . Electron heating was provided by a dc electric field of up to  $20 \text{ V cm}^{-1}$  applied across the sample. The ac sensing current of the bridge was always kept small enough that its contribution to heating was negligible.

The experiments were carried out with the samples attached to the inside bottom of a sealed copper chamber that was thermally coupled to a bath of helium. This arrangement provided a good thermal contact between the substrate and the helium bath whose temperature was controlled to better than 1 mK over the range 1–4.2 K. The chamber could either be evacuated or filled with liquid helium so that the exposed surface of the Au-Pd film was either in a vacuum or covered with liquid helium. This arrangement enabled electron-heating effects to be studied as a function of the phonon escape which could be modified *in situ*. To avoid the problems of a residual helium layer on the metal film, the experiments al-

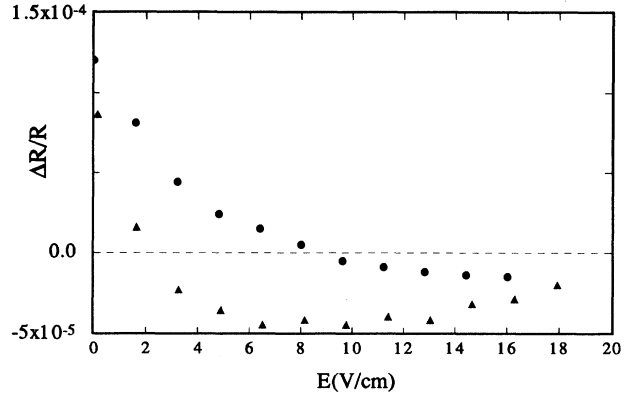


FIG. 2. The change in resistance vs electric field for the film in vacuum (▲) and immersed in helium (●).  $T_s = 1.7 \text{ K}$ .

ways started with the chamber evacuated. After helium was condensed into the chamber we did not attempt to go back to the evacuated conditions without warming the cryostat.

The equilibrium resistance change of the films as a function of temperature is shown in Fig. 1. A minimum resistance  $R_{0\text{eq}}$  is found at  $T_0 \approx 7 \text{ K}$  below which the resistance increases logarithmically. This resistance rise is consistent with the resistance corrections from electron-electron interactions and localization reported for similar films by other workers.<sup>13,14</sup> The corrections we observed were found to be reproducible on many samples. No change was found in the equilibrium temperature dependence of the resistance with the sample chamber evacuated or filled with liquid helium.

The response of the resistance change  $[R(E) - R_{0\text{eq}}]/R_{0\text{eq}} = \Delta R/R$  to an applied dc electric field  $E$  was very different when the surface of the film was in vacuum and in helium. As shown in Fig. 2, when the

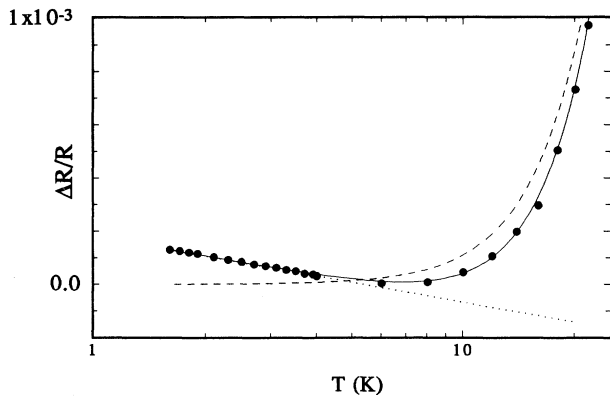


FIG. 1. The equilibrium temperature dependence of  $\Delta R/R$ . To within experimental error, data from the film in vacuum and in helium showed the same temperature dependence. The lines show a fit to the equilibrium data using the Drude (—) and interaction (···) contributions to the total resistance. The solid curve is the sum of the two contributions.

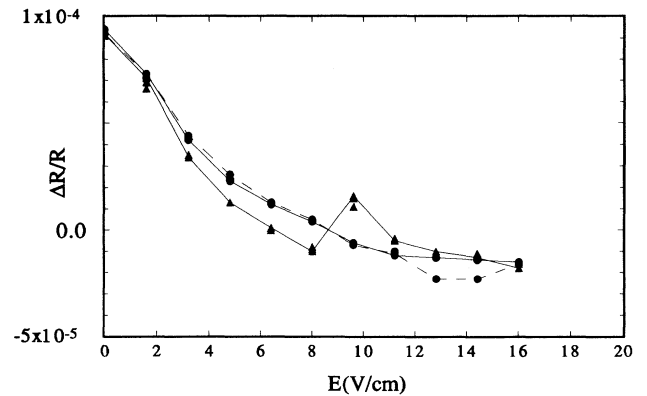


FIG. 3. The change in resistance vs electric field for  $T_s = 2.120, 2.140, 2.160, 2.180, 2.200,$  and  $2.220 \text{ K}$ . The data fall into two distinct groups, one for  $T_s > T_\lambda$  (▲) and the other  $T_s < T_\lambda$  (●). The curves are guides to the eye only. For  $T_s > T_\lambda$ , the feature at  $9 \text{ V cm}^{-1}$  is reproducible and for  $T_s$  just below  $T_\lambda$  the feature at  $13 \text{ V cm}^{-1}$  is reproducible.

film is covered with helium,  $\Delta R/R$  falls continuously over the whole range of applied electric fields. Conversely, for a film in vacuum the low-field behavior of  $\Delta R/R$  has a stronger dependence on the field, but at a field of approximately  $8 \text{ V cm}^{-1}$  it reaches a minimum and then increases. An important effect seen in Fig. 2 is that for both surface conditions  $\Delta R/R$  is reduced below zero as  $E$  increases; that is,  $R(E)$  becomes less than  $R_{0eq}$ . This effect has been reported previously,<sup>2</sup> but in the present and earlier<sup>3</sup> experiments we have observed that the amount by which the resistance falls below  $R_{0eq}$  depends on the nature of the medium above the free surface of the film. The form of  $R(E)$  was also found to depend on the state of the helium covering the film.

Figure 3 shows the change in  $\Delta R/R$  as the helium covering the film is changed from helium II to helium I by raising the temperature from 2.120 to 2.220 K in 20-mK steps across the lambda point  $T_\lambda = 2.172 \text{ K}$ . A strong feature was observed in the helium I data at  $\sim 9 \text{ V cm}^{-1}$ , as seen in Fig. 3 and shown in more detail in Fig. 4. Since we are measuring the ac resistance, this peak can be interpreted as the derivative of a step in the current-voltage characteristic of the film caused by the onset of helium boiling. The shoulder on the high-field side of the peak was reproducible. The power at which the strong feature occurred was found to be inversely proportional to the temperature of the helium. By a simple linear extrapolation to zero power, we obtain a temperature of  $6.0 \pm 0.8 \text{ K}$ , which is close to the critical temperature for helium and suggests the feature originates from helium boiling.

In the majority of reported experiments that have used an electric field to heat thin films, it has generally been assumed that the electrons are heated and that the phonons generated by the warm electrons escape from the film in a time less than the electron-phonon relaxation time. Thus the lattice temperature of the film is assumed to remain at the temperature of the substrate on which it is supported. This approximation implies that the escape of the phonons from the film will have no effect on  $R(E)$ . Our results demonstrate quite clearly that this is not the case and that phonon escape from the metal film must be taken into account in experiments that drive the electrons and phonons out of equilibrium with each other.

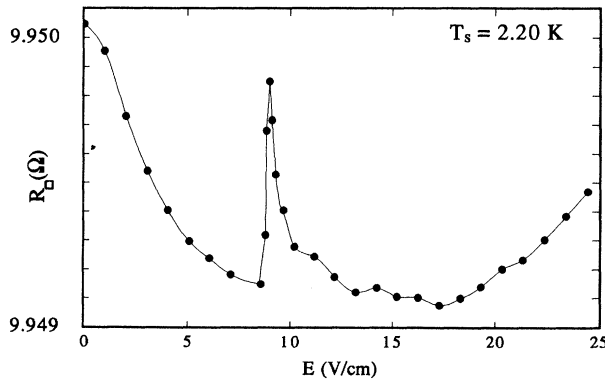


FIG. 4. A higher resolution sweep of the sharp feature at  $9 \text{ V cm}^{-1}$ .

### III. MODEL

We will first discuss how  $R(E)$  can fall below  $R_{0eq}$ . This can be understood by examining how the various components that contribute to the equilibrium temperature dependence of the resistance combine in the steady state:

$$R_{\text{tot}}(T_e, T_{\text{ph}}) = R_{\text{int}}(T_e) + R_{\text{wk}}(T_e, T_{\text{ph}}) + R_D(T_e, T_{\text{ph}}), \quad (1)$$

where the electron and phonon temperatures are  $T_e$  and  $T_{\text{ph}}$ , respectively, and the components are  $R_{\text{int}}(T_e)$ , an electron-electron interaction term;  $R_{\text{wk}}(T_e, T_{\text{ph}})$ , a weak localization term; and  $R_D(T_e, T_{\text{ph}})$ , a Drude term that includes both the electron-phonon inelastic lifetime  $\tau_{e\text{-ph}}^i$  and the scattering time of electrons  $\tau_e$  due to impurities. The logarithmic terms are given by the expressions<sup>15,16</sup>

$$R_{\text{int}} = -R_{\square}^2 \frac{e^2}{2\pi^2 \hbar} (1 - \frac{3}{4}F) \ln(T_e),$$

$$R_{\text{wk}} = -R_{\square}^2 \frac{e^2}{2\pi^2 \hbar} \ln(L_{\phi}), \quad (2)$$

where  $F$  is a screening parameter between 0 and 1, and  $L_{\phi}$  is the phase breaking length of the electrons that depends on  $T_e$  and  $T_{\text{ph}}$ .<sup>1</sup>

In equilibrium, the electron temperature is identical to the phonon temperature. At temperatures well above  $T_0$  the Drude term is dominant and since  $\tau_{e\text{-ph}}^i \propto T^{-\beta}$ , this provides a power-law dependence to the resistance  $R \propto T^{\beta}$ . In the present experiments we find  $\beta=3$ . At temperatures well below  $T_0$ , the Drude term becomes smaller than the other terms which provide the observed logarithmic resistance rise. For Au-Pd films and wires, Lin and Giordano<sup>14</sup> have shown that the interaction term is generally dominant, with  $F \approx 0.1$ . Leaving out the weak-localization term, the combination of the two remaining terms with  $F=0.15$  gives a resistance minimum in equilibrium, as shown in Fig. 1.

When a dc electric field is applied to the film the system comes to a steady state in which the electron temperature is greater than the phonon temperature which itself is generally above the substrate temperature  $T_s$ . We note that the phonon distribution in the film is not an equilibrium distribution and for the present discussion  $T_{\text{ph}}$  is an effective phonon temperature; we will return to this point in more detail later. On the other hand, we assume the electron-electron interaction is sufficiently strong to bring the electron system into internal equilibrium with a Fermi distribution characterized by  $T_e$ .

With the system in the steady state, the relative contribution of each term to the resistance is modified because they each have a different dependence on  $T_e$  and  $T_{\text{ph}}$ . For instance, if  $T_{\text{ph}}$  is held at  $T_s$  by perfect acoustic coupling between the film and substrate, the summation would be shown schematically in Fig. 5. In the other extreme, if  $T_{\text{ph}}$  and  $T_e$  increase together as the dc field is applied, then the sum of the terms will never be less than  $R_{0eq}$ . We will model the heating experiment by assuming that the resistance as a function of electric field  $R(E)$  can

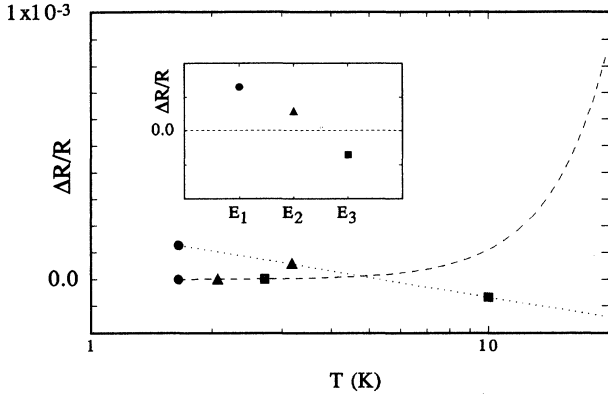


FIG. 5. The hypothetical resistance contributions at three electric fields  $E_1$ ,  $E_2$ , and  $E_3$  are represented by the three different symbols. As a result of the different temperature dependences of the resistance terms, the symbols appear at different temperatures for each term. To obtain the change of resistance with field, the contributions at a given field are summed, as demonstrated in the inset.

be obtained from equation 1 if  $T_e$  and  $T_{ph}$  are known as a function of the applied electric field.

For the case of an actual heating experiment, the steady-state temperatures of the electrons and phonons will depend on the details of the phonon generation by the heated electrons and the subsequent phonon escape from the metal film, which in turn depends on the particular metal/substrate combination used in the experiment. We have modeled this situation using an approach originally introduced by Perrin and Budd.<sup>17,18</sup> The rate equation

$$\frac{dn(\omega)}{dt} = \frac{n(\omega, T_e) - n(\omega)}{\tau_{e-ph}} + \frac{n(\omega, T_s) - n(\omega)}{\tau_{esc}} \quad (3)$$

is used to describe the relaxation of energy from the electron system to the phonon system in the film and subsequently to the substrate. The nonequilibrium phonon distributions is given by  $n(\omega)$ , and the Bose distributions of the phonons at the electron temperature and the substrate temperature are  $n(\omega, T_e)$  and  $n(\omega, T_s)$ , respectively. For moderate electric fields, two characteristic times are required to determine the relaxation of energy; the phonon escape time from the film to the substrate  $\tau_{esc}$  and the electron-phonon relaxation time  $\tau_{e-ph}$ . The escape time is taken to be of the form<sup>19</sup>  $\tau_{esc} = 4\eta d / \bar{v}$ , where  $\bar{v}$  is the average group velocity of the longitudinal and transverse modes given by  $3\bar{v}^{-3} = (v_L^{-3} + 2v_T^{-3})$  and  $\eta$  is a frequency-independent reflection coefficient equal to  $(2\Gamma)^{-1}$  in the notation of Little.<sup>5</sup>

The films used in the experiment were of low disorder. From the Drude formalism we estimate the elastic mean free path  $l$  for the electrons to be 4 nm. Taking the dominant phonon wave vector to be  $q = 2kT/\hbar\bar{v}$ , we find  $ql$  approximately equal to unity at the temperatures used in this work. Therefore we have taken the complete form of the Pippard<sup>20</sup> model to describe the electron-phonon interaction for both longitudinal and transverse modes:

$$\begin{aligned} \tau_L^{-1} &= \frac{Nm}{\rho_m \tau_e} \left[ \frac{1}{3} \frac{q^2 l^2 \tan^{-1}(ql)}{ql - \tan^{-1}(ql)} - 1 \right], \\ \tau_T^{-1} &= \frac{Nm}{\rho_m \tau_e} \frac{1-g}{g}, \end{aligned} \quad (4)$$

with

$$g = \frac{3}{2q^2 l^2} \left[ \frac{(q^2 l^2 + 1)}{ql} \tan^{-1}(ql) - 1 \right].$$

In these expressions  $N$  is the electron density,  $m$  is the electron mass,  $\rho_m$  is the mass density, and  $\tau_e$  is the elastic-scattering time of the electrons. To avoid the problem of having independent rate equations for each phonon mode, we have used an averaged  $\tau_{e-ph}$  given by the expression  $3(\tau_{e-ph})^{-1} = (\tau_{e-ph}^L)^{-1} + 2(\tau_{e-ph}^T)^{-1}$ .

Under the steady-state conditions of the present experiments, the power per volume being transferred from the film to the substrate is<sup>18</sup>

$$\frac{E^2}{\rho} = \int D(\omega) \hbar \omega \frac{n(\omega, T_e) - n(\omega, T_s)}{\tau_{e-ph} + \tau_{esc}} d\omega, \quad (5)$$

where  $\rho$  is the resistivity and  $D(\omega)$  is the Debye phonon density of states. The two characteristic times act in series and form a bottleneck in which the longest dominates the overall relaxation of energy from the film. Since it seems unlikely that the electrons in the film couple directly to the helium, the process of allowing helium into the chamber can be considered to introduce a new loss path for phonons that is in addition to the phonon escape into the substrate. The two routes for phonon loss act in parallel with the combined effect of reducing the phonon escape time from the film.

In the steady state the phonon distribution is obtained from Eq. (3) to be

$$n(\omega) = \frac{\tau_{e-ph} n(\omega, T_s) + \tau_{esc} n(\omega, T_e)}{\tau_{e-ph} + \tau_{esc}}.$$

Equating this nonequilibrium distribution to a Bose distribution we can assign a temperature at each frequency,

$$T(\omega) = \frac{\hbar \omega}{k_B \ln[n(\omega)^{-1} + 1]}.$$

From these temperatures we then define the effective phonon temperature to be the weighted average over all frequencies

$$T_{ph} = \frac{\int T(\omega) D(\omega) n(\omega) d\omega}{\int D(\omega) n(\omega) d\omega}.$$

Within the framework of the model, the calculation required to fit the data is relatively direct. For each set of data at a given substrate temperature, the integral in Eq. (5) is numerically evaluated for a series of electron temperatures above  $T_s$ . This yields the electric field required to heat the electrons to each  $T_e$ . Also for each value of  $T_e$ , an effective phonon temperature is calculated from the steady-state phonon distribution as described previously. At this point both the electron temperature and

an effective phonon temperature are known for each value of the electric field; that is, we have determined  $T_e(E)$  and  $T_{ph}(E)$ . These values are then used in Eq. (1) to yield the total resistance as a function of electric field.

Under steady-state conditions, it has been shown that  $\tau_{e-ph}^i$  depends on both  $T_e$  and  $T_{ph}$ .<sup>1,21</sup> This will affect the temperature dependence of  $R$  through the contributions from the Drude term. For small differences between the electron and phonon temperatures, we have used the approximation for the Drude temperature  $T_D = xT_e + (1-x)T_{ph}$ , where  $x$  is expected<sup>2</sup> to be near 0.3, and in the steady state  $R_D \propto T_D^\beta$ .

#### IV. DISCUSSION

The material parameters we have used for Au-Pd are a mass density  $\rho_m = 16400 \text{ kg m}^{-3}$ , an electron density  $N = 5.8 \times 10^{28} \text{ m}^{-3}$ , a Fermi velocity  $v_F = 1.4 \times 10^6 \text{ ms}^{-1}$ , and sound velocities  $v_L = 4.1 \times 10^3 \text{ ms}^{-1}$  and  $v_T = 1.8 \times 10^3 \text{ ms}^{-1}$ . The sound velocities were obtained from a weighted average of Au and Pd values.<sup>13</sup>

The fit parameters used are the phonon reflection coefficient  $\eta$  and the fraction  $x$  used to determine  $T_D$ . The fit parameters were evaluated by trial and error.

We will begin by discussing the fit to the resistance versus applied dc field data for the case when the sample is immersed in helium. Curve *A* in Fig. 6 shows the fit to the data taken at 1.7 K in helium using the fit parameters  $x = 0.1$  and  $\eta = 1.6$ . Changing the fit parameters in the range  $0 < x < 0.4$  and  $1 < \eta < 16$  did not substantially affect the quality of the fit. This lack of sensitivity on the fit parameters may be explained by the fact that within

these ranges  $T_D$  is low enough that the Drude contribution to the steady-state resistance is small.

To fit the data in the case when there is a vacuum above the free surface of the sample, one might expect that the removal of the phonon escape path into the helium would be represented by increasing  $\eta$  (i.e., the effective  $\tau_{esc}$ ) above the value found when helium was present. However, the situation is not that simple. As shown by curves *B*, *C*, and *D* in Fig. 6, if the escape time is increased, the low-field data do become steeper as required to fit the vacuum data, but at higher fields the fit becomes progressively worse. In our analysis of previous data<sup>10</sup> at relatively low fields, we used a frequency-dependent reflection coefficient to obtain a fit. The present data and fits show that such an analysis cannot be used at higher fields, because a frequency-dependent  $\eta$  would enhance the phonon trapping and make the fits even worse.

Since the material parameters used in the expression for  $\tau_{e-ph}$  [Eq. (4)] are not well characterized in thin films, we checked the fits after changing the magnitude of the relaxation time. For the film immersed in helium, the best fit was found with no change in the magnitude of  $\tau_{e-ph}$ . For the film in a vacuum, a fit was obtained with the magnitude of  $\tau_{e-ph}$  increased by a factor of 20. Since the same film was used under both surface conditions we believe this change in the magnitude of  $\tau_{e-ph}$  to be non-physical. In addition, we found that for no single value of the magnitude could both sets of data be fit by just changing the escape time.

From our analysis, using reasonable choices for the fit parameters, we conclude that the model using 3D phonons alone is unable to adequately explain both the data obtained with the film in helium and in vacuum.

We now discuss the possibility of 2D phonons in the films and modify the model to account for low-dimension phonon effects. When helium is coating the free surface of the film, the ratio of the sound velocities between helium and the metal shows that all the phonons in the film will couple into a narrow cone in the helium.<sup>7</sup> Since the acoustic coupling coefficient between the film and the helium is much larger than expected from the acoustic mismatch model, we anticipate that in this case the phonons in the film will be of three-dimensional character. However, when the film is in vacuum, only phonons with wave vectors inside the critical cone,  $\theta_{cr} \approx 30^\circ$  can escape into the substrate. These phonons are expected to be three dimensional, while those outside the critical cone are presumed to be two dimensional up to a frequency at which the phonon loses phase memory over the thickness of the film by undergoing an inelastic scattering event.

We have modeled the situation by splitting the integral in Eq. (5) into two parts, one describing three-dimensional phonons, the other two-dimensional phonons. The two-dimensional term includes the 2D density of states and is integrated up to a cutoff frequency  $\omega_c$  that is used as a fit parameter related to the inelastic phonon scattering in the film. The density of states we have used is the ideal 2D Debye density of states which is only strictly true for phonons with zero momentum perpendicular to the substrate. The functional form of  $\tau_{e-ph}$  for 2D

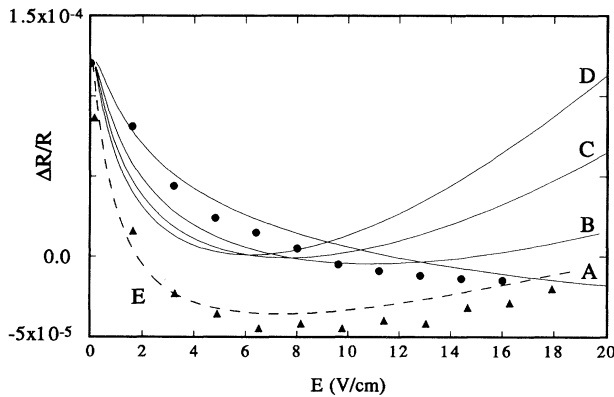


FIG. 6. The change in resistance vs electric field for the film in vacuum ( $\blacktriangle$ ) and immersed in helium ( $\bullet$ ). Curve *A* shows the fit to the data for the film immersed in helium using a 3D phonon spectrum and  $\eta = 1.6$ . The solid curves *B*, *C*, and *D* indicate attempts to fit the data for the film in a vacuum by only increasing the escape time from the value used for curve *A*. The values of  $\eta$  were 40, 80, and 120 for curves *B*, *C*, and *D*, respectively. Clearly, the low electric-field behavior changes in the correct direction, but the resistance change at high fields becomes greatly overestimated due to phonon trapping. The dashed curve *E* is a fit using a 2D+3D phonon spectrum.  $T_s = 1.7 \text{ K}$ .

phonons has been calculated by Belitz<sup>22,23</sup> to be

$$\begin{aligned}\tau_L^{-1} &= \frac{\pi}{12} \frac{Nmq^2 l^2}{\rho \tau_e} f_L(ql), \\ \tau_T^{-1} &= \frac{1}{4} \frac{Nmq^2 l^2}{\rho \tau_e} f_T(ql),\end{aligned}\quad (6)$$

where

$$f_L(x) = \frac{2}{\sqrt{(1+x^2)}} \left[ 1 + \frac{2}{x^2} - \frac{1}{\sqrt{(1+x^2)}-1} \right]$$

and

$$f_T(x) = \frac{8}{x^4} [x^2 - \sqrt{(1+x^2)} + 1],$$

and is shown in Fig. 7 along with the Pippard expressions. It is seen that the 2D and 3D functional forms are similar, except for the transverse mode at high frequencies. For the 2D cases, we have used an averaged  $\tau_{e-ph}$  given by the expression  $2(\tau_{e-ph})^{-1} = (\tau_{e-ph}^L)^{-1} + (\tau_{e-ph}^T)^{-1}$  that accounts for the loss of one transverse mode. To be consistent we have also used a 2D average sound velocity given by  $2\bar{v}^{-2} = (v_L^{-2} + v_T^{-2})$ . The 2D phonons have wave vectors outside the critical cone and may not escape directly from the film. However, as mentioned in the Introduction, scattering into the critical cone will open an escape route to the 2D phonons. This introduces another bottleneck between the time to scatter into the critical cone and  $\tau_{esc}$  for the 3D phonons. For simplicity, we assume this bottleneck to be dominated by  $\tau_{esc}$  and so introduce  $\tau_{esc}$  into the term describing the 2D phonons.

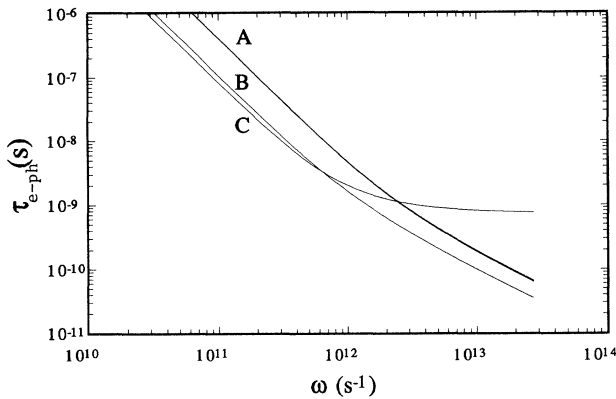


FIG. 7. The frequency dependence of  $\tau_{e-ph}$  in Au-Pd. Curves A and B are calculated from the Pippard model for longitudinal and transverse phonons, respectively, with the two transverse modes having the same velocity. The case for 2D phonons is calculated from Eq. (6). The relaxation time for longitudinal phonons is almost indistinguishable from that obtained from the Pippard model, curve A. At low frequencies the single transverse mode, curve C, has a similar magnitude and the same frequency dependence as the degenerate transverse modes in three dimensions. However, at high frequencies the 2D model predicts a much weaker frequency dependence for the transverse mode.

The fit to the vacuum data, curve E in Fig. 6, was obtained by using two-dimensional phonons below  $\omega_c = 1 \times 10^{13} \text{ s}^{-1}$  and three-dimensional phonons above. For this fit  $\eta$  was 3.2, and the prefactor to  $\tau_{e-ph}$  was the same as was used in the 3D fit to the helium. These values are in agreement with the idea that the addition of the helium only changes the phonon dimensionality and escape time and does not change the electron-phonon interaction. The cutoff frequency is found to be consistent with the relaxation length of three phonon processes,<sup>24,25</sup>  $l_{ph} = C\omega^{-5}$ , where  $C$  depends on the second- and third-order elastic constants of the material. Equating  $l_{ph}$  with the thickness of the film, we can estimate the phonon frequency below which anharmonic processes will be less likely than boundary scattering; thus we can obtain an estimate of  $\omega_c$ . Unfortunately, a direct comparison to a Au-Pd film is not possible since the elastic constants required to calculate  $C$  are not available for Au-Pd. Therefore we have used the constants for gold<sup>26,27</sup> and obtain  $\omega_c \approx 4 \times 10^{13} \text{ s}^{-1}$ , which is comparable to the value we found by fitting the data.

As mentioned above, to obtain fits to the data we needed to calculate  $T_e$  and  $T_{ph}$  as a function of  $E$ . For the parameters used to fit the helium and vacuum data, curves A and E in Fig. 6, respectively, the field dependence of  $T_e$  and  $T_{ph}$  is shown in Fig. 8. As expected, when the film is immersed in helium the electrons and phonons heat less rapidly with field than when the film is in vacuum; this is a consequence of both the change in the phonon escape time and the phonon spectrum.

Finally, we return briefly to the difference in the heating data that occurs when the helium covering the film becomes superfluid (Fig. 3). This difference may be understood qualitatively within the framework of the present model as a change in  $\tau_{esc}$  suggesting that under the experimental conditions described the thermal boundary resistance to helium II is less than the resistance to helium I. However, a quantitative analysis is complicated by the phase change of the helium from a superfluid to a classical hydrodynamic fluid. To account for this

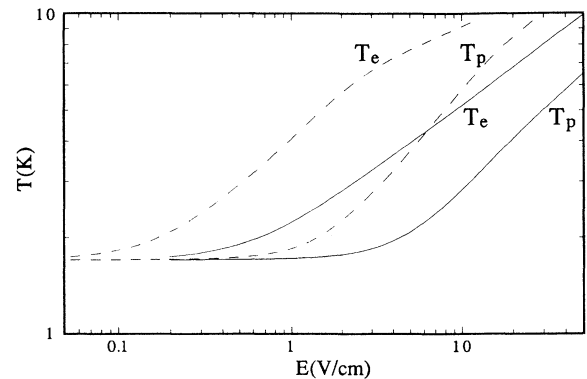


FIG. 8. The variation of  $T_e$  and  $T_{ph}$  with electric field for the film immersed in helium (solid curves) and in vacuum (dashed curves).

change of state, an extra term must be added to Eq. (3) to describe the heat transport in the helium itself. The effect of this term will be small when the film is immersed in helium II because the high thermal conductivity of the helium makes the bath an extremely good heat sink with very small thermal gradients. However, it may become important when the film is immersed in helium I because the much lower thermal conductivity will allow thermal gradients to be setup that will add an extra process in series with the electron-phonon and phonon escape processes.

### V. CONCLUSION

We have shown that the change in resistance of a metal film that is heated by an electric field is sensitive to the acoustic conditions at the film's surface. By considering

the system in the steady state, we have demonstrated that to within the physical range of the various parameters involved, the data cannot be explained with a simple 3D spectrum of phonons in the film. In a preliminary way we have extended the model to include the possibility of 2D phonon effects and have shown that this modified phonon spectrum considerably improves the fit to the data.

### ACKNOWLEDGMENTS

We would like to thank D. Belitz for many useful discussions on electron-phonon coupling and for providing us with the unpublished results given in Eq. (6). This work was supported by the National Science Foundation under Grant No. DMR-87-13884.

- 
- <sup>1</sup>G. Bergmann, Wei Wei, Yao Zou, and R. M. Mueller, Phys. Rev. B **41**, 7386 (1990).
  - <sup>2</sup>J. Liu, T. L. Meisenheimer, and N. Giordano, Phys. Rev. B **40**, 7527 (1989).
  - <sup>3</sup>J. C. Nabity and M. N. Wybourne, Phys. Rev. B **42**, 9714 (1990).
  - <sup>4</sup>B. A. Auld, *Acoustic Fields and Waves* (Wiley, New York, 1973), Vol. 2, Chap. 9.
  - <sup>5</sup>W. A. Little, Can. J. Phys. **37**, 334 (1959).
  - <sup>6</sup>C. Höss, J. P. Wolfe, and H. Kinder, Phys. Rev. Lett. **64**, 1134 (1990).
  - <sup>7</sup>A. F. G. Wyatt, G. J. Page, and R. A. Sherlock, Phys. Rev. Lett. **36**, 1184 (1976).
  - <sup>8</sup>J. M. Pfotenhauer and R. J. Donnelly, Adv. Heat Transfer **17**, 65 (1985).
  - <sup>9</sup>E. T. Swartz and R. O. Pohl, Rev. Mod. Phys. **61**, 605 (1989).
  - <sup>10</sup>J. C. Nabity and M. N. Wybourne, J. Phys. Condens. Matter **2**, 3125 (1990).
  - <sup>11</sup>J. C. Nabity and M. N. Wybourne, Rev. Sci. Instrum. **60**, 27 (1989).
  - <sup>12</sup>M. V. Moody, J. L. Paterson, and R. L. Ciali, Rev. Sci. Instrum. **50**, 903 (1979).
  - <sup>13</sup>W. C. McGinnis and P. M. Chaikin, Phys. Rev. B **32**, 6319 (1985).
  - <sup>14</sup>J. J. Lin and N. Giordano, Phys. Rev. B **35**, 545 (1987).
  - <sup>15</sup>B. L. Altshuler, A. G. Aronov, and P. A. Lee, Phys. Rev. Lett. **44**, 1288 (1980).
  - <sup>16</sup>E. Abrahams, P. W. Anderson, D. C. Licciardello, and T. V. Ramakrishnan, Phys. Rev. Lett. **42**, 673 (1979).
  - <sup>17</sup>N. Perrin and H. Budd, Phys. Rev. Lett. **28**, 1701 (1972).
  - <sup>18</sup>N. Perrin and H. Budd, J. Phys. (Paris) Colloq. **33**, C4-33 (1972).
  - <sup>19</sup>W. E. Bron and W. Grill, Phys. Rev. B **16**, 5303 (1977).
  - <sup>20</sup>A. B. Pippard, Philos. Mag. **46**, 1104 (1955).
  - <sup>21</sup>P. B. Allen, Phys. Rev. Lett. **59**, 1460 (1987).
  - <sup>22</sup>D. Belitz (private communication).
  - <sup>23</sup>D. Belitz and S. Das Sarma, Phys. Rev. B **36**, 7701 (1987).
  - <sup>24</sup>S. Tamura, Phys. Rev. B **31**, 2574 (1985).
  - <sup>25</sup>A. Berke, A. P. Mayer, and R. K. Wehner, J. Phys. C **21**, 2305 (1988).
  - <sup>26</sup>J. R. Neighbours and G. A. Alers, Phys. Rev. **111**, 707 (1958).
  - <sup>27</sup>B. P. Barua and S. K. Sinha, J. Appl. Phys. **49**, 3967 (1978).